Electronic Supplementary Material (ESI) for Chemical Communications

Evidence for magnetic anisotropy of $[Nb^{IV}(CN)_8]^{4-}$ in pillared-layered Mn_2Nb framework showing spin-flop tranisition

Electronic Supplementary Information

Dawid Pinkowicz*,[a] Michał Rams,[b] Wojciech Nitek,[a] Bernard Czarnecki[a] and Barbara Sieklucka

* pinkowic@chemia.uj.edu.pl

Table of Contents:

Section 1: Synthetic procedure

Chemicals and solvents used in this study were purchased from commercial sources (Aldrich) and used without further purification. 4,4'-bipyridyl-N,N'-dioxide was purchased from Sigma-Adrich as a hydrate bpdo·xH_2O and used as received. Potassium octacyanoniobate(IV) dihydrate $K_4[Nb(CN)_8]\cdot 2H_2O$ was prepared according to literature procedures.[1]

Synthesis of $\{[Mn^{II}_2(bpdo)(H_2O)_4][Nb^{IV}(CN)_8]\cdot 6H_2O\}_n$ **Mn(bpdo)Nb**. Aqueous solutions of $MnCl_2\cdot 4H_2O$ (6 ml, 0.040 g, 0.2 mmol) and bpdo (6 ml, 0.080 g, approx. 0.4 mmol) were mixed and added to an aqueous solution of $K_4[Nb(CN)_8]\cdot 2H_2O$ (10 ml, 0.052 g, 0.1 mmol). The resulting slightly turbid yellow solution was left to stand for about 24 hours in the dark at room temperature for crystallization. After this time yellow needle-like single crystals approximately 1 mm long were isolated from the mother liquor by repeated decantation, washed with cold water, dried shortly using filter paper and stored in a closed vessel at -20°C. The mother liquor was left to stand for few more days and the additional portions of the product were collected. Yield ca. 40 mg (50%); Anal. calc. (%) for $C_{18}H_{28}Mn_2N_{10}NbO_{12}$: C, 27.74; H, 3.62; N, 17.97. Found: C, 27.98; H, 3.19; N, 18.10.

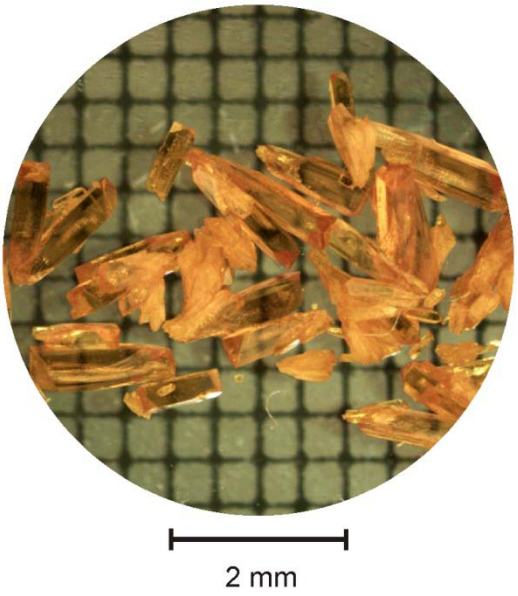

Section 2: Crystallographic details

The single crystal diffraction data were collected at room temperature on a Nonius Kappa CCD diffractometer. The space group was determined using ABSEN.[2] The structure was solved by direct methods using SIR-97.[3] Refinement and further calculations were carried out using SHELXL-97.[4] The non-H atoms were refined anisotropically using weighted full-matrix least-squares on F^2. Hydrogen atoms joined to C atoms of bpdo ligand were positioned with an idealized geometry and refined using riding model with U_{iso}(H) fixed at 1.2U_{eq}(C). All hydrogen atoms joined to oxygen atoms of crystallization and coordination water were found from the difference Fourier map and then refined using a riding model (AFIX 3) with U_{iso}(H) fixed at 1.5U_{eq}(O). 15 restraints have been employed in the refinement of the molecular geometry of water molecules: O-H and H-O-H distances have been fixed at 0.900 and 1.470 Å, respectively (details have been included in the crystallographic information file). Table S1 shows the detailed crystallographic data.

Table S1. XRD data collection and refinement details for $\{[Mn^{II}_2(bpdo)(H_2O)_4][Nb^{IV}(CN)_8]\cdot 6H_2O\}_n$ **Mn(bpdo)Nb**

	Mn(bpdo)Nb
method	single-crystal XRD
instrument	Nonius Kappa CCD
formula	$C_{18}H_{28}Mn_2N_{10}NbO_{12}$
FW [$g\cdot mol^{-1}$]	779.29
crystal system	orthorhombic
space group	P 2_12_12
unit cell dimensions [Å]	*a* = 10.4925(1)
	b = 11.4782(1)
	c = 12.3333 (2)
V [$Å^3$]	1485.36(3)
Z	2
d_{calcd} [$g\cdot cm^{-3}$]	1.742
T [K]	298
abs. coeff. [mm^{-1}]	1.290
abs. corr. type	Multi-scan
max/min transmission	0.827/0.683
F (000)	786
wavelenght [Å]	0.71073
cryst. size [mm]	0.30 × 0.10 × 0.10
range for data collection [deg]	$2.42 \le \vartheta \le 34.97$
index ranges	$-16 \le h \le 16$
	$-17 \le k \le 18$
	$-19 \le l \le 19$
reflections collected	19735
completeness of θ [%]	99.9
refinement method	full matrix least-squares on F^2
weighting scheme	$w = 1/[\sigma^2(F_o^2) + (\alpha P)^2 + \beta P]$,
	where $P = (F_o^2 + 2F_c^2)/3$
data/restraints/parameters	6512/15/239
GOF	1.076
R indices (reflections)	R_1 = 0.0282 (5824)
	wR_2 = 0.0649 (6512)
Flack parameter	-0.009(13)
largest diff. peak and hole	0.679/-0.515

Figure S1. The pillared-layered organic-inorganic coordination framework of $\{[Mn^{II}_2(bpdo)(H_2O)_4][Nb^{IV}(CN)_8]\cdot 6H_2O\}_n$ viewed along *a*, *b* and *c* crystallographic axes (2-D cyano-bridged Mn_2Nb layers in red, 1-D -Mn_2-bpdo-Mn_2- chains in green).

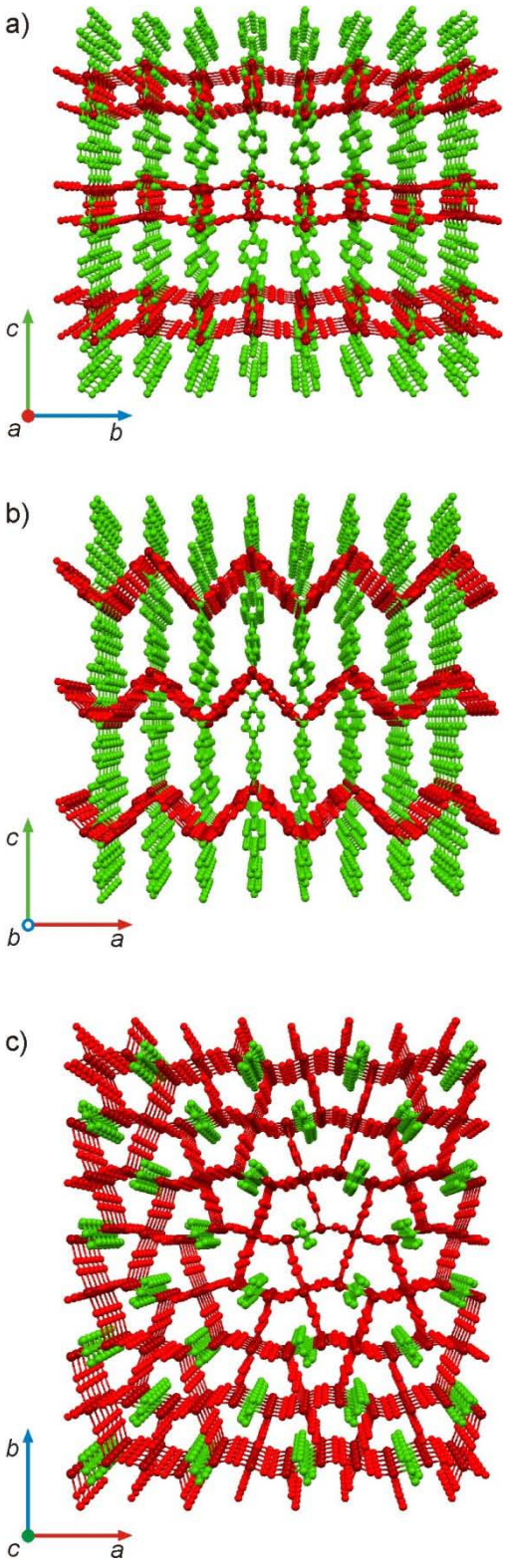

Figure S2. The 5-metallic hybrid ring - the basic structural motif of the inorganic layers a), the basic structral motif of the metal-organic chains b), coordination sphere and connectivity of the Nb center c) and coordination sphere and connectivity of the Mn center d) in **Mn(bpdo)Nb** (Mn-pink, Nb-orange, C-gray, N-blue, O-red, H-white; label „a“ denotes 2-fold proper rotation axis related atoms and „b“ denotes 2-fold screw axis related atoms; ellipsoid probability at 50%).

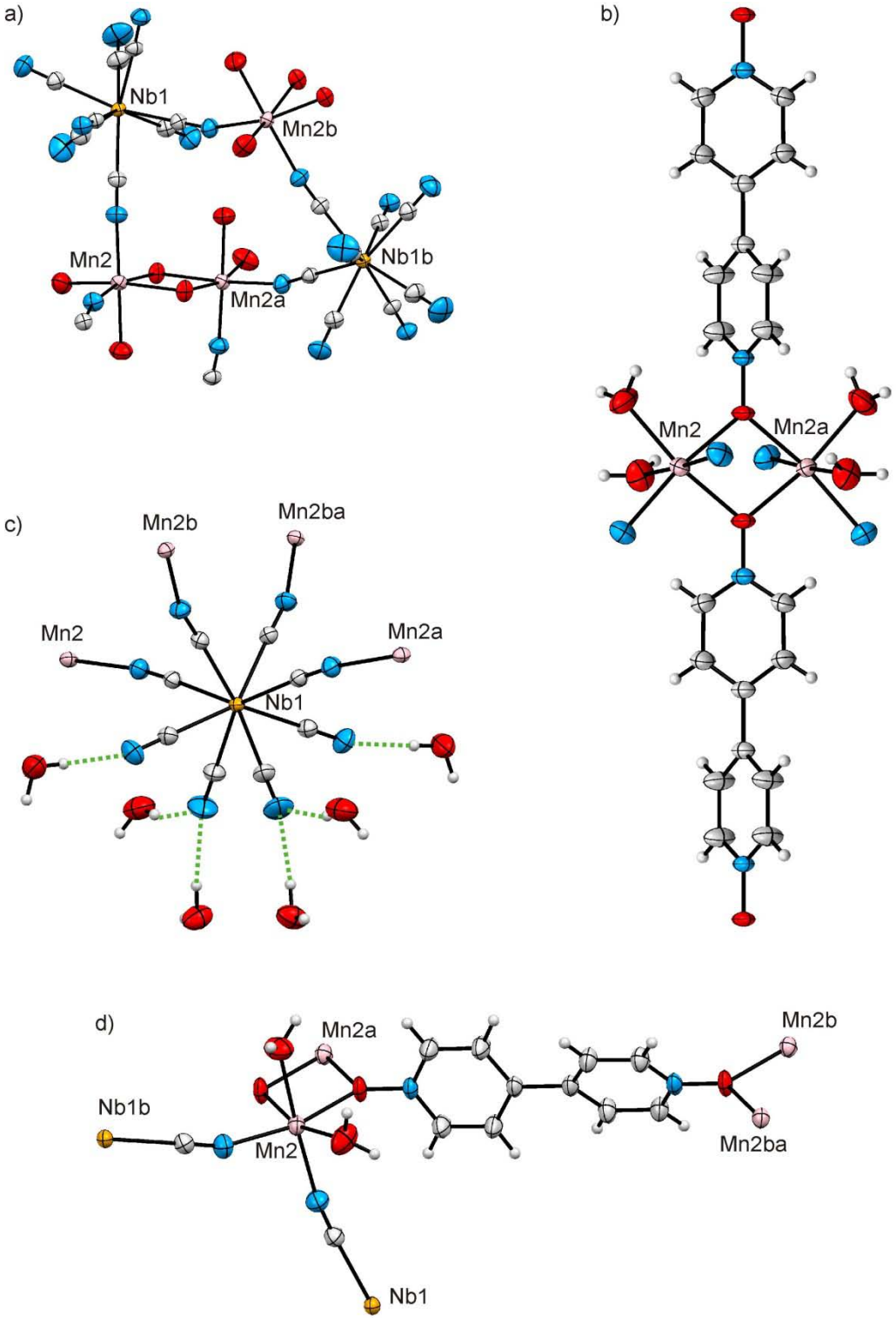

Table S2. Continuous Shape Measure (CShM) Analysis[a] for the coordination spheres of Nb^{IV} and Mn^{II} in **Mn(bpdo)Nb**

Coordination sphere of Mn^{II}

	OC[*]	**TP**[**]	Mn in **Mn(bpdo)Nb**
S_{OC}	0	ca. 16	0.94
S_{TP}	ca. 16	0	13.76
$\Delta_{OC\text{-}TP}$	0	0	13.2%
$\boldsymbol{\varphi_{TP\rightarrow OC}}$	100%	0%	**90.2%**
$\varphi_{OC\rightarrow TP}$	0%	100%	23.0%
judgement			**OC geometry slightly distorted towards TP**

[*] octahedron, [**] trigonal prism
[a] S_{OC}, S_{TP} - shape measure relatives to the OC and TP, respectively (equal to 0 if the real geometry coincides with the idealized one); $\Delta_{OC\text{-}TP}$ represents the deviation from the OC-TP interconversion path; $\varphi_{A\rightarrow B}$ - Angular Path Fractions: equal to 0 when the real geometry coincides with A and equal to 100 for B.

Coordination sphere of Nb^{IV}

	DD[*]	**SAPR**[**]	Nb in **Mn(bpdo)Nb**
S_{DD}	ca. 2.8	0	2.04
S_{SAPR}	0	ca. 2.8	0.19
$\Delta_{DD\text{-}SAPR}$	0	0	10.4%
$\varphi_{SAPR\rightarrow DD}$	100%	0%	25.8 %
$\boldsymbol{\varphi_{DD\rightarrow SAPR}}$	0%	100%	**84.6 %**
judgement			**SAPR geometry slightly distorted towards DD**

[*] triangular dodecahedron, [**] square antiprism,
[a] S_{DD}, S_{SAPR} - shape measure relatives to the DD, SAPR, respectively (equal to 0 if the real geometry coincides with the idealized one); $\Delta_{DD\text{-}SAPR}$ represents the deviation from the DD-SAPR interconversion path; $\varphi_{A\rightarrow B}$ - Angular Path Fractions: equal to 0 when the real geometry coincides with A and equal to 100 for B.

Geometry of the coordination sphere of Nb^{IV} perpendicular to (a) and along (b) its 4-fold symmetry axis

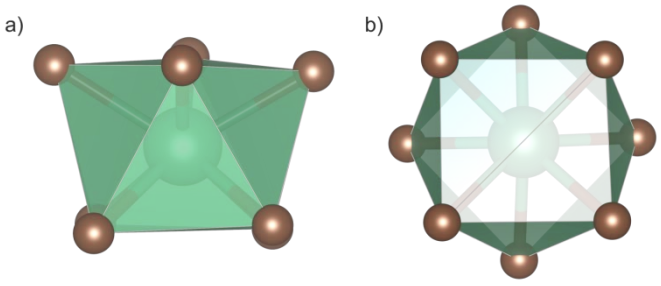

Table S3. Metric parameters of selected bonds and angles in **Mn(bpdo)Nb**

	Bond lengths [Å]		Angles [deg]		M-M distances [Å]	
Nb1	Nb1-C11	2.258(2)	Nb1-C11-N11	177.1(2)	Nb1-Mn2	5.521
	Nb1-C12	2.241(2)	Nb1-C12-N12	179.0(2)	Nb1-Mn2	5.604
	Nb1-C13	2.273(2)	Nb1-C13-N13	177.1(2)		
	Nb1-C14	2.234(2)	Nb1-C14-N15	179.4(2)		
Mn2	Mn2-N11	2.182(2)	Mn2-N11-C11	162.0(2)		
	Mn2-N13	2.212(2)	Mn2-N13-C13	170.7(2)		
	Mn2-O5	2.218(1)	O5-Mn-O10	72.9(1)	Mn2-Mn2	3.563
	Mn2-O10	2.211(1)				
	Mn2-O1H	2.138(1)				
	Mn2-O2H	2.233(1)				

Figure S3. Fragment of the structure of **Mn(bpdo)Nb** with atom labeling scheme (ellipsoid probability at 50%).

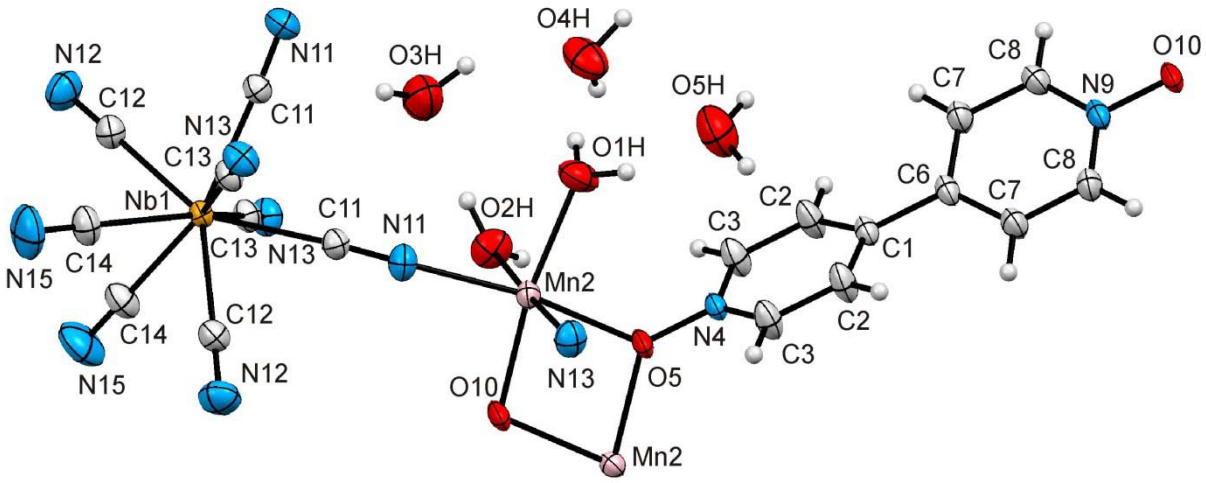

Figure S4. Helical structural motifs within the inorganic layers viewed along *a* direction (2-fold screw axis; only Nb-CN-Mn and Mn-O-Mn linkages are shown; bpdo, H_2O and terminal CN omitted for clarity).

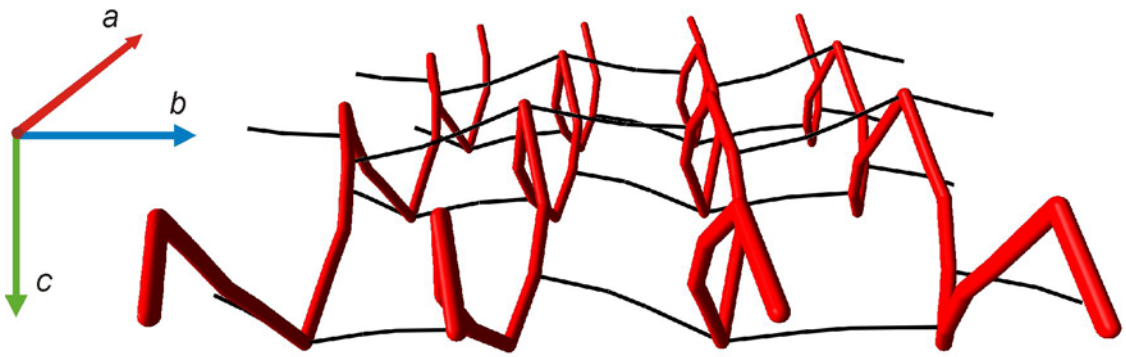

Figure S5. IR spectra of **Mn(bpdo)Nb** (blue line), $K_4[Nb^{IV}(CN)_8]\cdot 2HO$ (red line) and commercially available bpdo ligand (green line) with short description (below).

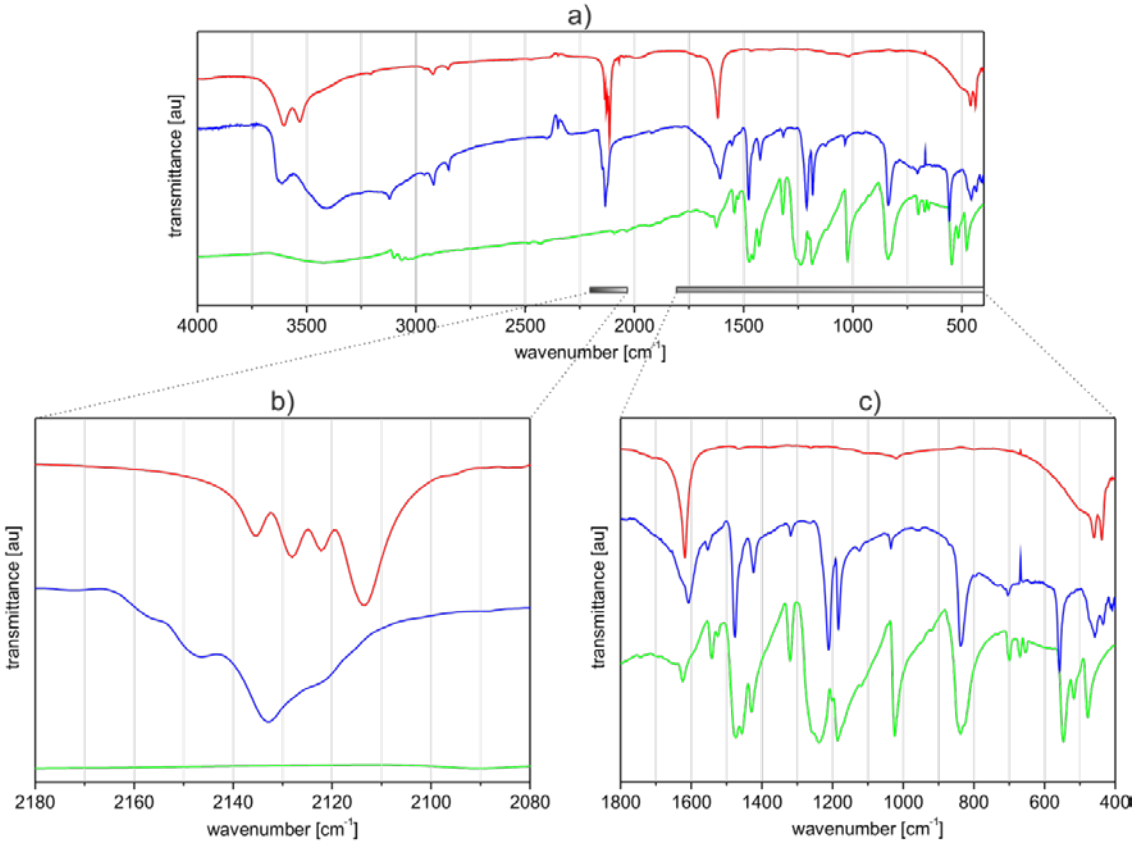

Both spectra of **Mn(bpdo)Nb** and pure bpdo show strong, wide bands in O-H (3600-3000cm^{-1}) and C-H stretching region (3000-2800cm^{-1}) and are very similar in the fingerprint region (1800-400cm^{-1}). This confirms the presence of bpdo in **Mn(bpdo)Nb**. The "blue shift" of the C≡N band s in **Mn(bpdo)Nb** (2121sh, 2132vs, 2146m, 2156sh cm^{-1}) compared to $K_4[Nb^{IV}(CN)_8]\cdot 2H_2O$ (2113vs, 2121m, 2128m and 2135w cm^{-1}) strongly suggest the formation of Mn-CN-Nb linkages.

Figure S6. Experimental (red line, shifted) and simulated (gray line) PXRD patterns of **Mn(bpdo)Nb**

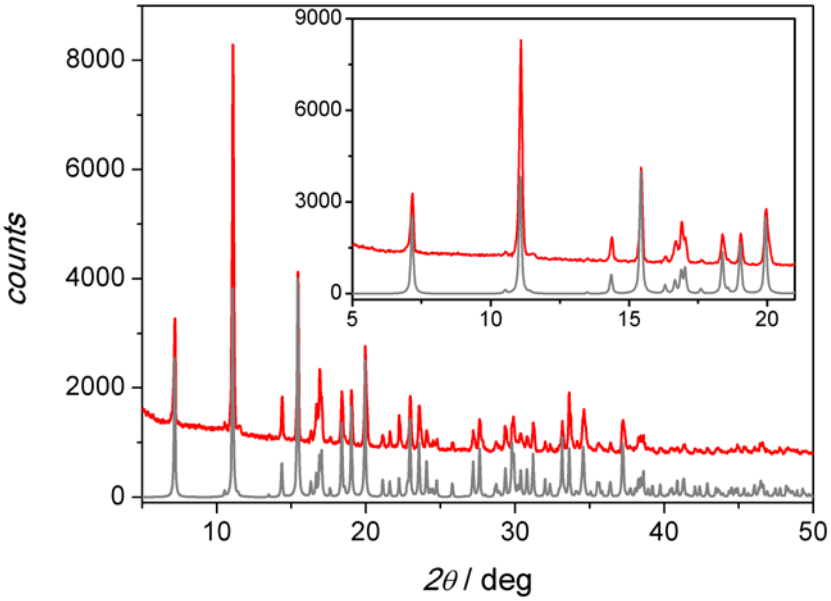

Figure S7. Thermogravimetric analysis of **Mn(bpdo)Nb** (black line) with QMS lines corresponding to the decomposition products: water (blue line) and hydrogen cyanide (violet line).

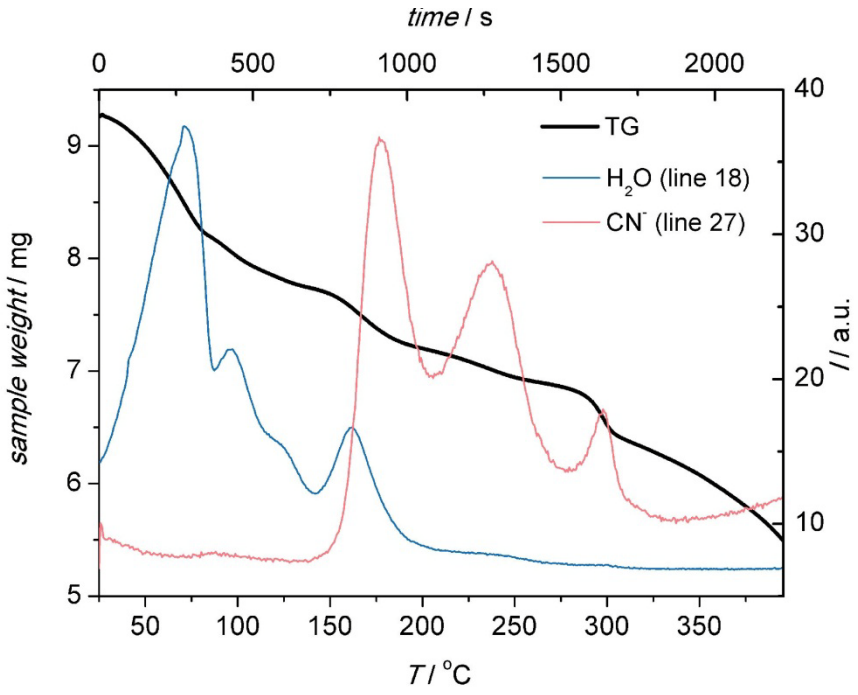

Figure S8. Time dependent PXRD experiments at standard temperature and pressure showing the transformation of the crystal structure of **Mn(bpdo)Nb** upon dehydration. The first 9 scans have been performed one after another with total experiment time of 90 minutes, the last scan (black line) was performed after the sample was left in ambient air at room temperature for 2 days.

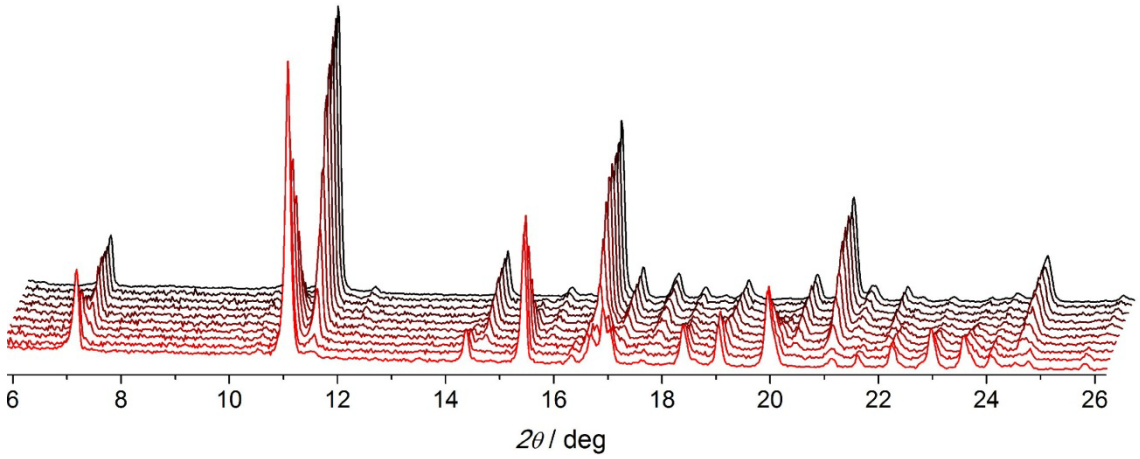

Figure S9. $X^{-1}(T)$ plot for **Mn(bpdo)Nb** fitted to Curie-Weiss law (green line) and molecular field theory (red line). For details see text.

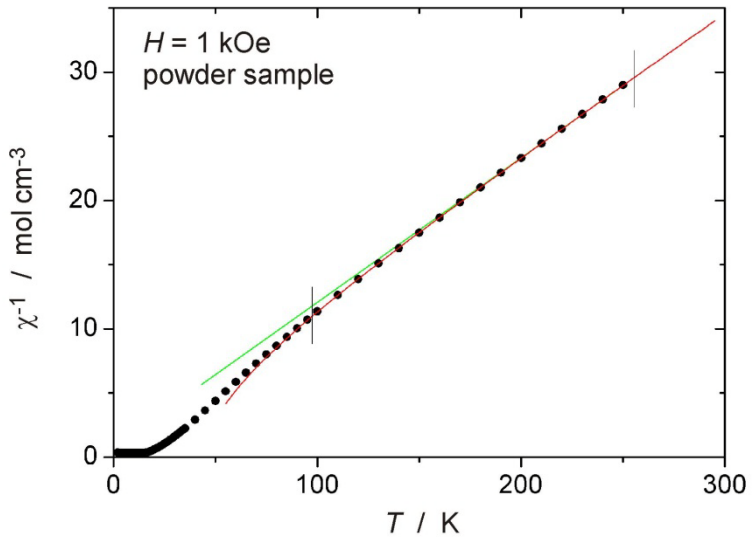

Figure S10. The magnetic susceptibility of **Mn(bpdo)Nb** measured at different fields along *a* axis

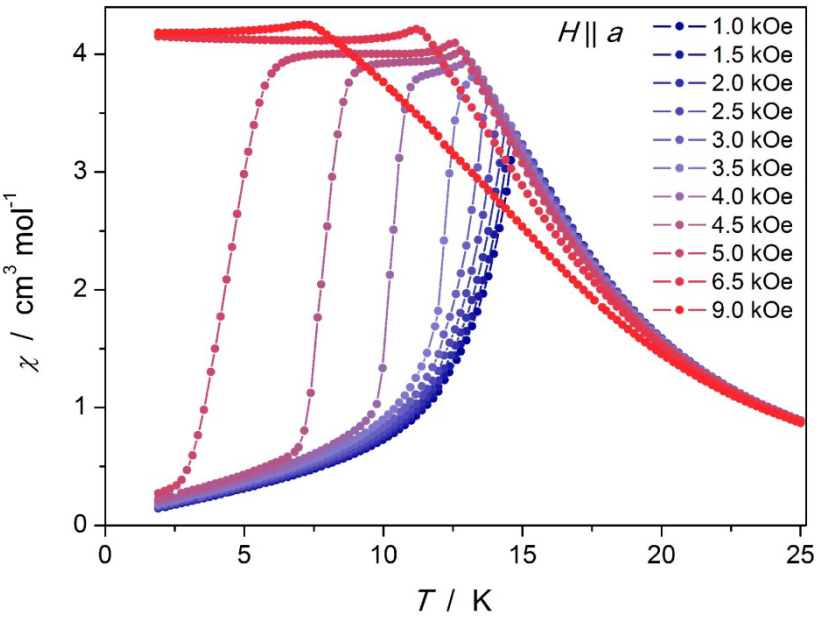

Figure S11. Structural diagram showing fragment of the **Mn(bpdo)Nb** framework along *c* axis and the alignement of the local 4-fold symmetry axes of $[Nb^{IV}(CN)_8]$-moieties.

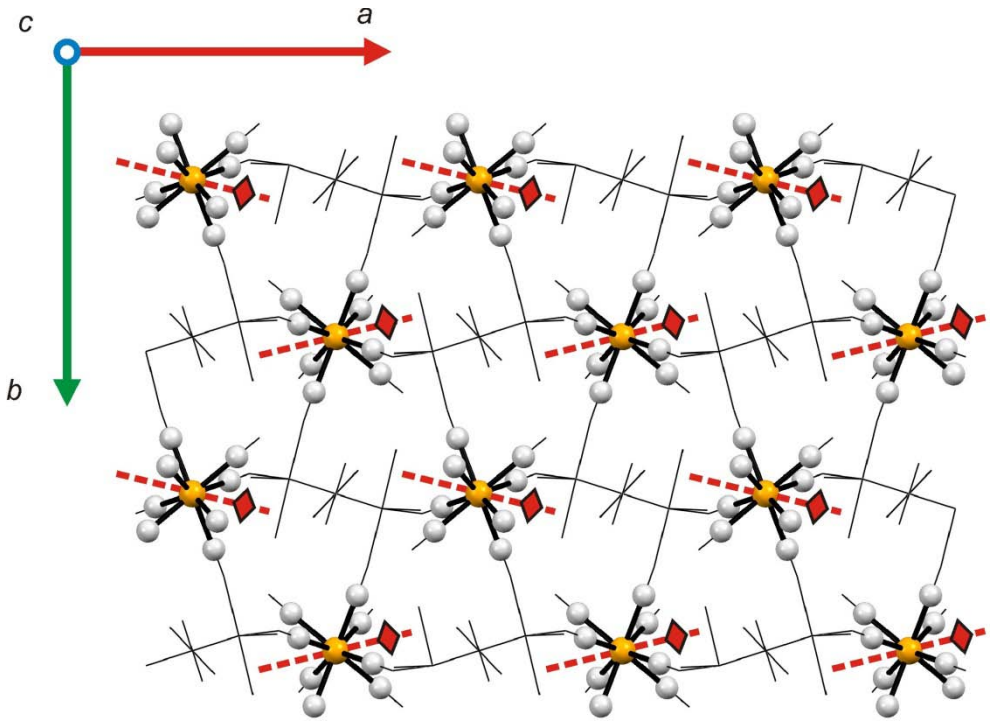

References in Electronic Supplementary Information

[1] a) P. M. Kiernan, J. F. Gibson, W. P. Griffith, *J. Chem. Soc. Chem. Commun.* 1973, 816-817; b) P. M. Kiernan, W. P. Griffith, *J. Chem. Soc., Dalton Trans.* 1975, 2489-2494
[2] P. *J.* McArdle, *Appl. Crystallogr.* 1996, **29**, 306
[3] A. Altomare, M. C. Burla, M. Camalli, G. L. Cascarano, C. Giacovazzo, A. Guagliardi, A. G. G. Moliterni, G. Polidori, R. Spagna, *J. Appl. Crystallogr.* 1999, **32**, 115
[4] G. M. Sheldrick, *Acta Cryst.* 2008, **A64**, 112-122